

Reconstruction of the Distal Radius Facet by a Free Vascularized Osteochondral Autograft: Anatomic Study and Report of a Patient

Francisco del Piñal, MD, Francisco J. García-Bernal, MD,
Julio Delgado, MD, Marcos Sanmartín, MD, Javier Regalado, MD,
Santander, Spain

Purpose: Large chondral defects of the distal radius after fractures present a reconstructive challenge. The purpose of this study was to present the anatomic findings from a cadaver of a vascularized osteochondral autograft taken from the third metatarsal appropriate for reconstructing the distal radius articular facet. A patient is presented in whom 70% of the scaphoid fossa was reconstructed with this technique.

Methods: The base of the third metatarsal was studied in the feet of 20 cadavers. The size and shape of the cartilage were measured. Additionally vessel distribution was recorded and the diameters of vascular foramina were measured with Juch's method.

Results: The base of the third metatarsal is pear shaped and is wider dorsally than plantarly. It averages 19.2 mm long on its main axis. Its cartilaginous surface is minimally concave or flat and it is slanted slightly proximal-dorsal to distal-plantar and proximal-peroneal to distal-tibial. Nutrient foramina were found in every case in the dorsum and on both sides of the proximal shaft. At least 1 nutrient vessel could be tracked back to the dorsalis pedis in every dissected specimen.

Conclusions: The anatomic features of the base of the third metatarsal make it a potential vascularized autograft to consider for osteochondral defects of the distal radius. (*J Hand Surg* 2005; 30A:1200.e1–1200.e14. Copyright © 2005 by the American Society for Surgery of the Hand.)

Key words: Osteochondral defects, intra-articular distal radius malunion, distal radius osteotomy, free flap.

From the Instituto de Cirugía Plástica y de la Mano, Hospital Mutua Montañesa and Clínica Mompía, Santander, Spain.

Received for publication March 10, 2005; accepted in revised form July 6, 2005.

No benefits in any form have been received or will be received from a commercial party related directly or indirectly to the subject of this article.

Supported in part by a grant from the Mutua Montañesa (Mutua de Accidentes de Trabajo y Enfermedades Profesionales de la Seguridad Social No. 7).

Corresponding author: Dr. Francisco del Piñal, MD, Calderón de la Barca 16-entlo, E-39002-Santander, Spain e-mail: pacopinal@ono.com.

Copyright © 2005 by the American Society for Surgery of the Hand 0363-5023/05/30A06-0014\$30.00/0

doi:10.1016/j.jhsa.2005.07.005

Note: To access the supplementary materials accompanying this article, visit the November 2005 issue of *Journal of Hand Surgery* at www.jhandsurg.org

Cartilage defects have been a challenge to researchers since at least 1743 when Hunter set the axiom, "Cartilage once injured is incapable of healing." The literature abounds with reports dealing with different methods to repair cartilage defects, from cultured chondrocyte autografts,¹ nonvascularized osteochondral autografts,^{2–11} mosaicplasty,¹² and fresh and frozen allografts^{13,14} to perichondrial resurfacing arthroplasty,^{15–19} none of them totally successful.^{5–7,9,12,13,17,18,20,21} Some of the failures may be due to the fact that both the anatomy of hyaline cartilage, and the relationships of the cartilage and subchondral bone, are extremely complex and difficult to reproduce.²²

It has been said that cartilage gets its nutrition

through diffusion from the synovial fluid and that it does not need a blood supply to survive.^{23–25} Nevertheless, several long-term studies on vascularized joint transfers in the hand literature confirm that the joint space is maintained over the years provided the blood supply to the joint is, however, preserved.^{26–28} Conversely the joint may collapse and the cartilage disappear if it is transferred as a nonvascularized graft.^{29–31} Furthermore recent evidence points to a major role of the subchondral bone interface in the nutrition of cartilage, at least of the deep layers.^{22,32} Therefore it seems logical to assume that the blood supply is important for cartilage nutrition and joint integrity.

Bone has been shown to maintain its mechanical and biological properties when distantly transferred, provided its blood supply is restored by microvascular anastomoses.^{33,34} By preserving its epiphyseal blood supply growth has been shown to occur when the transfer includes an open growth plate.^{35–37} Furthermore small blocks of metaphyseal bone that are nourished by tiny periosteal vessels have been used profusely in the care of difficult nonunions and avascular necrosis of carpal bones.^{38,39} In fact, any type of tissue or composite group of tissues can be transferred as a block from one part of the body to another provided its nutrient artery and its corresponding vein can be isolated and repaired in the recipient side.^{40,41}

A segment of cartilage taken together with its underlying vascularized subchondral bone would maintain the properties of the articular cartilage and also would maintain the complex anatomic relationships at the bone-cartilage interface. This article presents the anatomic findings of the base of the third metatarsal, relating its role as a donor site suitable for restoring the distal surface of the radius. In addition we present a patient whose scaphoid fossa was reconstructed by means of a vascularized osteochondral autograft.

Material and Methods

Anatomic Study

Eight fresh and 12 fresh-frozen feet were used to study the anatomy of the base of the third metatarsal. Ages ranged from 24 to 86 years with a median of 64 years. No major foot deformities were present. Dissections were performed under $\times 3.5$ loupe magnification. After elevation of the skin and retraction of the extensor tendons the vessels directed to the base of the second and third metatarsals were dissected and tracked back to their parent vessels. Measure-

ments of their calibers and the distance to the origin on the dorsalis pedis were performed. The presence of an arcuate artery or any other substantial vessels also was recorded.

The metatarsals then were cut at their proximal shaft and dissected *en bloc* by dividing all the soft-tissue attachments. The size, disposition, and location of the main and accessory articular surfaces were recorded. The distance from the most dorsal point of the articular surface and the inflexion point or flare (ie, the transition point between the widest and narrowest width) also were recorded. Measurements were taken with a Vernier caliper and the data were rounded to the nearest 1 mm or 0.1 mm as appropriate. Photographic records were used to calculate the surface by a computerized program (Volmed 2D; Informedia Designs, Leeds, UK). The slant of the articular surfaces on the coronal and sagittal planes were calculated with software (measuring instrument of Adobe Photoshop version 8.0.1; Adobe Systems Inc., San Jose, CA).

The specimens then were immersed in 100% bleach until all soft tissues were digested (approximately 2 hours). The locations of the vascular foramina were recorded and their diameters were calibrated by nylon sutures by Failla's⁴² modification of Juch's method. The technique consists of cannulating each foramen with increasing sizes of smooth monofilament suture representing a range of diameters (0.05–0.35 mm) from size 7-0 to size 0.

Results

Morphologic Data

The proximal surface of the third metatarsal was triangular to pear shaped, wider dorsally than plantar (dorsal width, 12.6 mm; range, 16–10 mm; plantar width, 7.9 mm; range, 10–5 mm), with an inflexion point located 8.7 mm from the most dorsal aspect of the base of the third metatarsal (Table 1). Its maximum dorsoplantar length averaged 19.2 mm (range, 21–17 mm). The third metatarsal proximal surface was flat (15 of 20 specimens) or slightly concave (5 of 20 specimens). It was slanted distally from dorsal to plantar and from fibular to tibial. The tibial tilt averaged 5° (range, 2°–10°) and the plantar tilt averaged 4° (range, 3°–7°). The cartilage surface averaged 167.6 mm² (range, 117–212 mm²) (Fig. 1).

The third metatarsal always has lateral facets: 2 in the tibial side and 1 in the fibular side. The former were irregular but the latter was notable for sigmoid notch reconstruction (see Discussion section). This fibular facet was located in the most dorsal aspect of

Table 1. Morphologic Parameters of the Third Metatarsal Base in 20 Specimens

Parameters	Mean	Minimum	Maximum
Dorsoplantar length	19.2	17	21
Width of dorsal aspect	12.6	10	16
Width of plantar aspect	7.9	5	10
Inflexion point (from dorsal aspect)	8.7	7	10
Dorsotibial facet DP*	5.5	4	7
Dorsotibial facet PD†	6.1	5	9
Plantotibial facet DP*	5.8	4	7
Plantotibial facet PD†	5.2	2	10
Fibular facet DP*	7.8	7	10
Fibular facet PD†	8.6	7	11
Articular area (mm ²)	167.6	117	212

Values in mm.
*PD, proximal-to-distal
†DP, dorsal-to-plantar.

the third metatarsal base and averaged 7.8 (dorsoplantar) by 8.6 mm (distal-proximal) wide (range, 7–10 and 7–11 mm wide, respectively). The accessory facet was flat and slightly tilted toward the tibial side.

Vascular

The third metatarsal has a dual dorsal blood supply: the distal lateral tarsal artery and the arcuate artery (Table 2). We were able to find an arcuate artery in 17 specimens, with its branching point located 10 mm distal to the third cuneometatarsal joint. The distal lateral tarsal artery branched from the dorsalis

Table 2. Vascular Parameters Related to the Third Metatarsal Blood Supply in 20 Uninjected Specimens

	Mean	Minimum	Maximum
Dorsalis pedis artery diameter	2.1	1.3	2.8
Arcuate artery diameter	0.5	0.2	0.9
Distal lateral tarsal artery diameter	0.6	0.4	1.0
Arcuate to third CMT*	10‡	4	15
DLTA to third CMT†	18.9	13	23

Values in mm.

CMT, cuneo-metatarsal joint.

*Distance from the arcuate artery to the third cuneometatarsal joint. Note the take-off of the arcuate artery always is distal to the base of the third metatarsal.

†Same from the distal lateral tarsal artery. Note that the take-off of the distal lateral tarsal artery always is proximal.

‡Absent in 3 specimens.

pedis at an average of 19 mm proximal to the base of the third metatarsal. The latter was the dominant artery in 13 of 20 specimens whereas in 7 specimens the arcuate was the major artery (Fig. 2).

Vascular foramina were found in every specimen and in each of the sides (dorsal, tibial, fibular). The larger were located on the sides in the vicinity of the accessory facets. On the dorsum there always were at least 3 foramina (range, 3–6) with a caliber that varied from 0.35 to 0.15 mm (Table 3).

Case Report

A 33-year-old man sustained a comminuted intra-articular fracture caused by a high-energy fall that

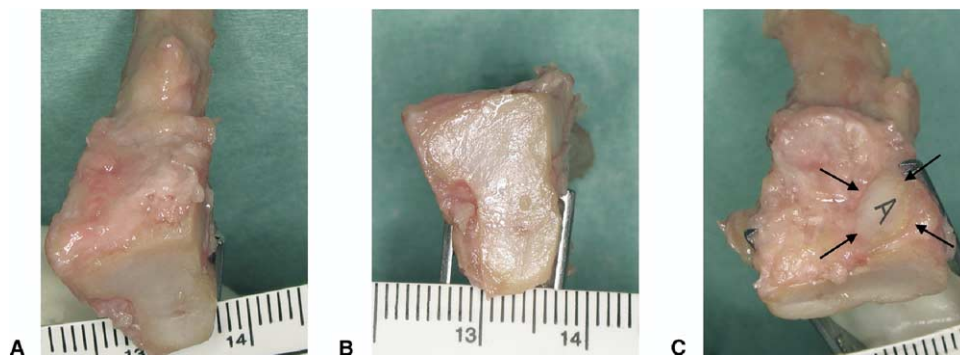


Figure 1. Anatomic features of the base of the left third metatarsal. (A) Dorsal view to appreciate the slight inclination of the principal facet distally from dorsal to plantar and from fibular to tibial. (B) Proximal (principal) facet. (C) Accessory (peroneal) facet.

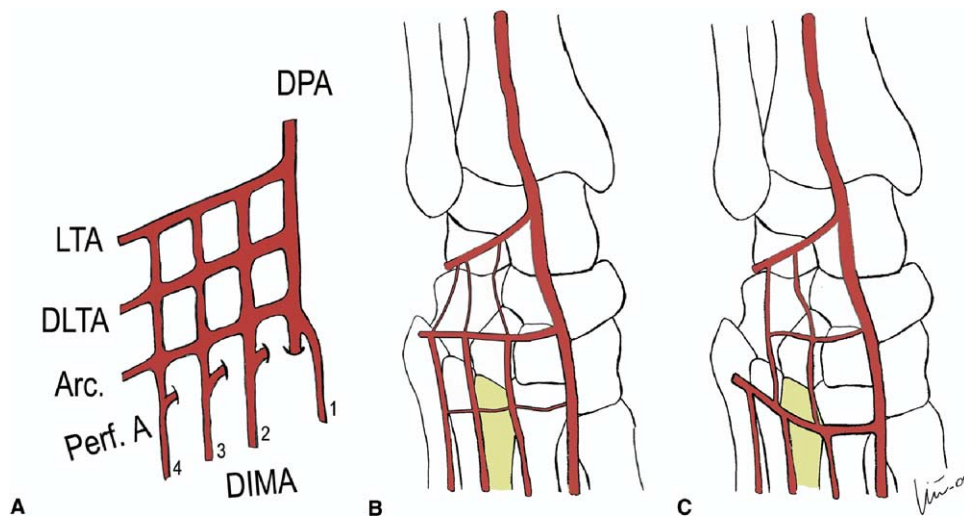


Figure 2. The blood supply to the dorsum of the foot and the variations most commonly found in this study (see text for more detail). (A) Classic arterial network. DPA, dorsalis pedis; LTA, lateral tarsal artery; DLTA, distal lateral tarsal artery; ARC, arcuate vessels; PERF A, perforating arteries; DIMA, dorsal intermetatarsal arteries. (B) Distal lateral tarsal artery dominance (the arcuate vessels are hypoplastic or absent). (C) Arcuate artery dominance (the distal lateral tarsal are hypoplastic or absent).

initially was treated with a palmar 3.5-mm T plate (AO/ASIF; Synthes, Oberdorf, Switzerland). Despite rehabilitation, 6 months later the patient continued to complain of pain and limited motion (extension, 5°; flexion, 35°; grip, 31% of contralateral side; pain on visual analog scale = 9 [0 = no pain; 10 = maximum pain]). X-rays and computed tomography scans showed destruction of the scaphoid fossa (Fig. 3).

The wrist was approached through a longitudinal midline incision, the extensor pollicis longus was released from its compartment, and the tendons of the second and fourth compartments were dissected subperiostically. The capsule was dissected from the dorsal rim of the radius and the posterior interosseous nerve was divided. Except for the dorsally angulated palmar margin the rest of the scaphoid fossa was found scarred, shattered, and devoid of cartilage. The scaphoid's proximal pole was covered by acceptable-looking cartilage (otherwise the procedure would have been aborted and a salvage surgery would have

been performed).⁴³ An external fixator (AO) was applied and the wrist was distracted. All scarred bone and cartilage were removed. Metaphyseal bone was excised as necessary to create a 3-dimensional space for the base of the third metatarsal. The palmar rim of the radius, which contained the radioscaphocapitate and long radiolunate ligaments, was cut and leveled to the lunate fossa; local bone graft was packed under this fragment for support. The actual cartilage defect corresponded to approximately 70% of the scaphoid fossa.

Graft Harvesting Technique

After exsanguination by elevation, a zigzag incision located between the extensor digitorum longus and the extensor hallucis longus allowed isolation of the dorsalis pedis artery and venae comitantes. A cutaneous perforator was dissected to nourish a skin island that was 3 × 1 cm, later to be used as a graft monitor. The extensor digitorum longus was retracted laterally and the extensor hallucis brevis tendon was divided to expose fully the vascular tree of the dorsum of the foot (Fig. 4).

The exact location of the base of the third metatarsal was ascertained with fluoroscopy. We found a small distal lateral tarsal and a larger arcuate artery directed toward the base of the third metatarsal; both vessels were included to nourish the bone. The distal lateral artery and any other tiny suprapariosteal vessel were protected by including a cuff of periosteum. The third metatarsal was cut distal to the arcuate artery and dissected from its ligamentous attach-

Table 3. Size Distribution of Vascular Foramina of the Third Metatarsal Base

Size (mm)	Tibial Side	Fibular Side	Dorsal Side
0.35	11	16	4
0.30	7	8	9
0.25	13	14	18
0.20	19	17	36
0.15	11	13	24

Absolute values of the 20 specimens.

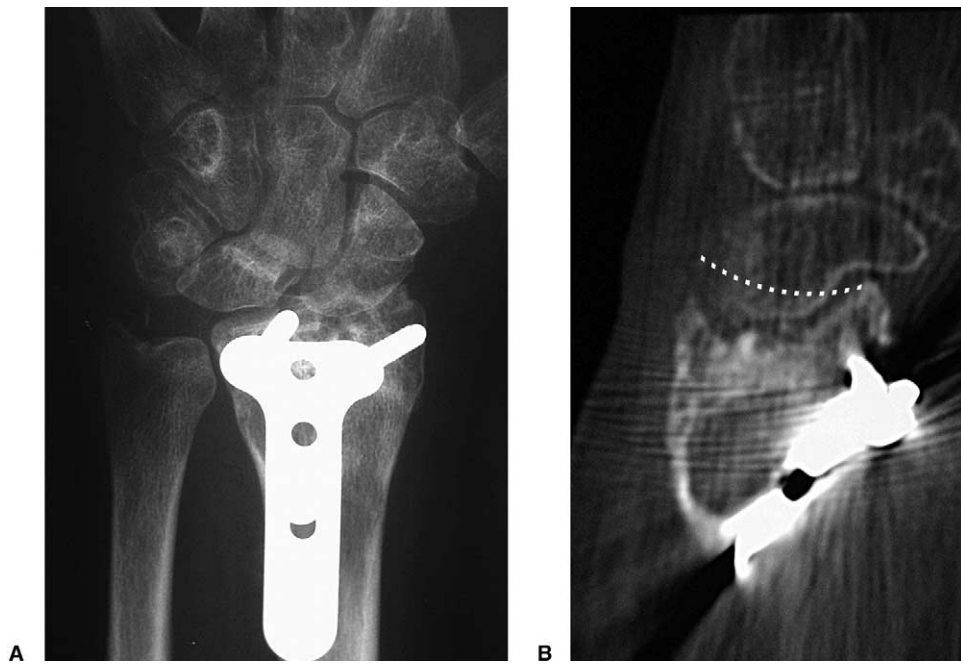


Figure 3. (A) Preoperative plain posteroanterior radiograph and (B) sagittal computed tomography scan. Normal contour in white dots.

ments until it could be pedicled on its nutrient vessels. The intermetatarsal space is very tight and the intermetatarsal ligaments are very deep. Rough maneuvers may put the nutrient vessels at risk: a lamina spreader was invaluable in this part of the surgery to separate the metatarsals. The first dorsal metatarsal artery then was ligated distal to the take-off of the

arcuate artery and the deep arterial branch to the plantar system also was divided. The graft then was isolated on the dorsalis pedis vessels (Fig. 5). The tourniquet was released, bleeding was appreciated from all the bone surfaces, and the skin monitor showed good capillary refill (video 1 can be viewed online at www.jhandsurg.org).

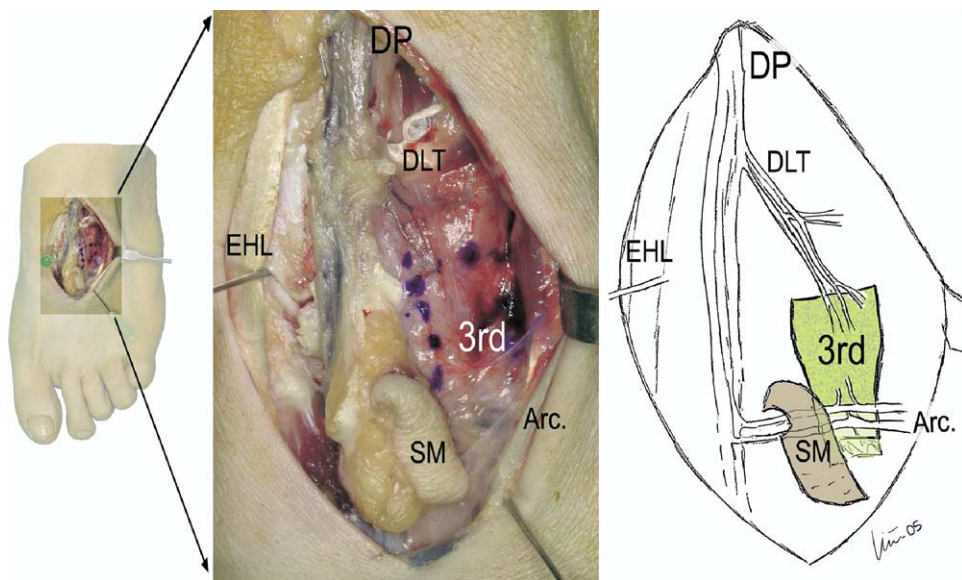


Figure 4. Flap harvesting. Detail of the vessel disposition on the dorsum of the foot in relation to the third metatarsal (left panoramic view). DP, dorsalis pedis; DLT, distal lateral tarsal; ARC, arcuate vessels; EHL, extensor hallucis longus; SM, skin monitor.



Figure 5. The graft now is elevated fully except for the dorsalis pedis vessels (arrow). It has been rotated cranially 180° for showing the proximal (principal) facet that articulates with the third cuneiform (P) and the accessory facet to the fourth metatarsal (A). SM, skin monitor.

Graft Transfer

The graft was taken to the hand. The peroneal cortex of the metatarsal was removed with a saw so there would be a cancellous surface against the radius. Once an even cartilage surface was achieved the osteochondral graft was fixed by 2.7-mm lag screws to the anterior radial cortex. The capsule was not repaired. The graft was revascularized by anastomosing the dorsalis pedis end-to-side to the radial artery

and a vena comitantes was anastomosed end-to-side to a subcutaneous vein. Profuse bleeding from the periosteum again was noted. The skin was closed in layers, leaving the skin island as a monitor. The external fixator was in place for 4 weeks and the wrist was in a splint for 2 more weeks. Rehabilitation was started at 8 weeks.

At 8 months, (Fig. 6) despite minimal pain on a visual analog scale (score, 1.5), the patient wished to improve the range of motion (active range of motion: extension, 20°; flexion, 45°). Arthroscopic arthrolysis was performed. The complete integrity of transferred cartilage with normal resiliency was noticed during exploration. In addition when the screws were removed percutaneously under arthroscopic guidance bleeding of the subchondral bone and normal adherence of the cartilage and bone were noticed (Fig. 7, video 2 can be viewed online at www.jhandsurg.org). At the latest follow-up evaluation 13 months after surgery the flexion was 50°, extension was 42°, radial deviation was 15°, and ulnar deviation was 28°. Grip strength was 78% of the contralateral side. The pain score on the visual analog scale was 1.5, and the score was 12 for the Disabilities of the Arm, Shoulder, and Hand questionnaire.⁴⁴ No surgery is planned nor is surgery expected on the wrist (video 3 can be viewed online at www.jhandsurg.org).

The foot skin was closed in a single layer with a drain in the metatarsal space. Without any attempt to



Figure 6. (A) Plain posteroanterior radiograph and (B) sagittal computed tomography scan 8 months after surgery. Arrows highlight the anterior portion of the vascularized osteochondral autograft.

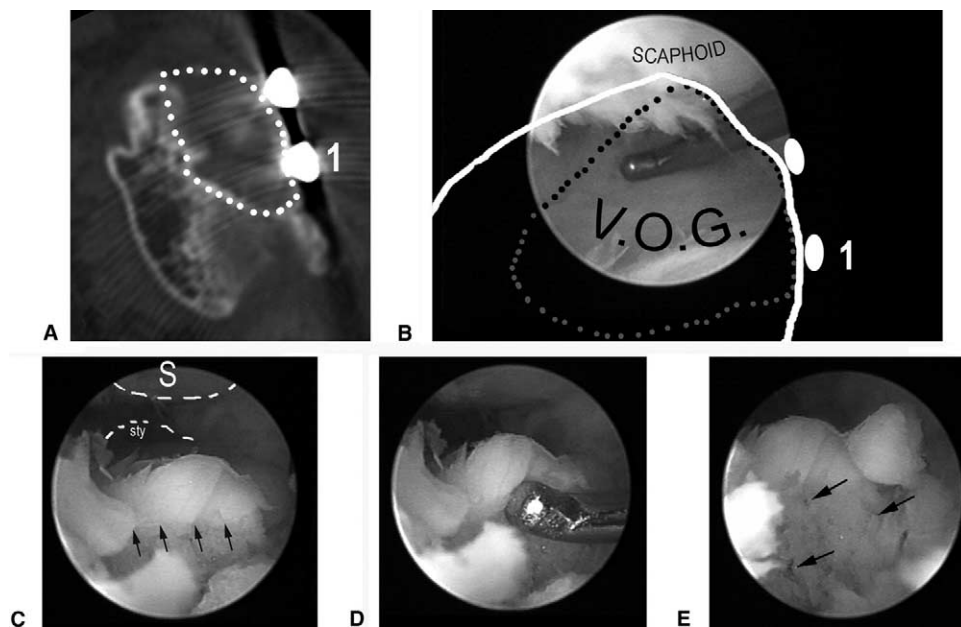


Figure 7. Arthroscopic findings at 8 months (see also video; this supplementary material can be viewed at the *Journal's* Web site, www.jhandsurg.org). 2). Outlines of the vascularized osteochondral graft (VOG) have been marked with red dots on the (A) axial computed tomography scan and the (B) arthroscopic panoramic view (outline of the radius in blue, screw head positions are represented by orange circles). (C–E) Scope is at 6-R portal looking at the dorsal edge of the osteochondral graft and focusing on the bone canal left by the screw that was fixing the graft. (This spot corresponds to “1” in A and B.) The scaphoid is above (s) on the very far end is the radial styloid (STYL). (C) Normal cartilage and subchondral bone interface (small arrows). (D) The probe is testing for delamination and is attempting to separate the cartilage from the subchondral bone by pushing distally. (E) Bleeding points on the canal left after removal of the screw are highlighted with red arrows.

reconstruct the metatarsal a plantar splint was applied for 3 weeks. Primary healing occurred and full weight-bearing ambulation was allowed at 6 weeks. At 1 year the patient complained of some soreness at the proximal aspect of the surgical scar that bothered him most when using tight shoes. This was interpreted as a neuroma of the deep peroneal nerve.⁴⁵ The patient nevertheless stated that he can walk for several kilometers. The gait pattern was normal and he tiptoed without difficulty. There were no complaints of metatarsalgia and no tenderness over the plantar aspect of the metatarsal heads. The American Orthopaedic Foot and Ankle Society rating system⁴⁶ to the lesser toes was applied and the patient scored 85 out of 100 points.

Discussion

Rapid degeneration of the radiocarpal joint is expected to occur after major intra-articular malunion.⁴⁷ This in part is caused by overload on the unaffected fossa⁴⁸ and because the malunited fragments erode the opposing surface of the carpal bone.^{47,49} Early osteotomy for impending malunion is advised and good results have been reported.^{50–52} When, however, the malunion involves more than 3

fragments or when arthritis is present, then osteotomies are no longer recommended.^{50–52}

Radiolunate arthrodesis is indicated only when damage is limited to the lunate fossa of the radius; an average of 66° of flexion–extension arc has been reported.⁵³ The radioscapolunate arthrodesis has stood the test of time but only an average flexion–extension arc of 40° can be provided in 50% of patients in the long term.⁵⁴ Garcia-Elias and Lluch⁵⁵ and McCombe et al⁵⁶ independently showed a marked improvement in the range of motion (27° on average) by excising the scaphoid's distal pole without an increase in degeneration at the midcarpal joint.⁴³ Panarthrodesis has the obvious disadvantage of loss of motion.

Reconstruction of cartilage defects is common in other fields of orthopedic surgery and various ways of approaching the problem have been published. Several institutions have the technology to perform fresh allogenic osteochondral grafting with good results reported.¹³ Despite the fact that survival of chondrocytes and chondral matrix is superior to the one seen in preserved allograft^{14,57} the signs of degeneration are appreciated in pathologic samples as

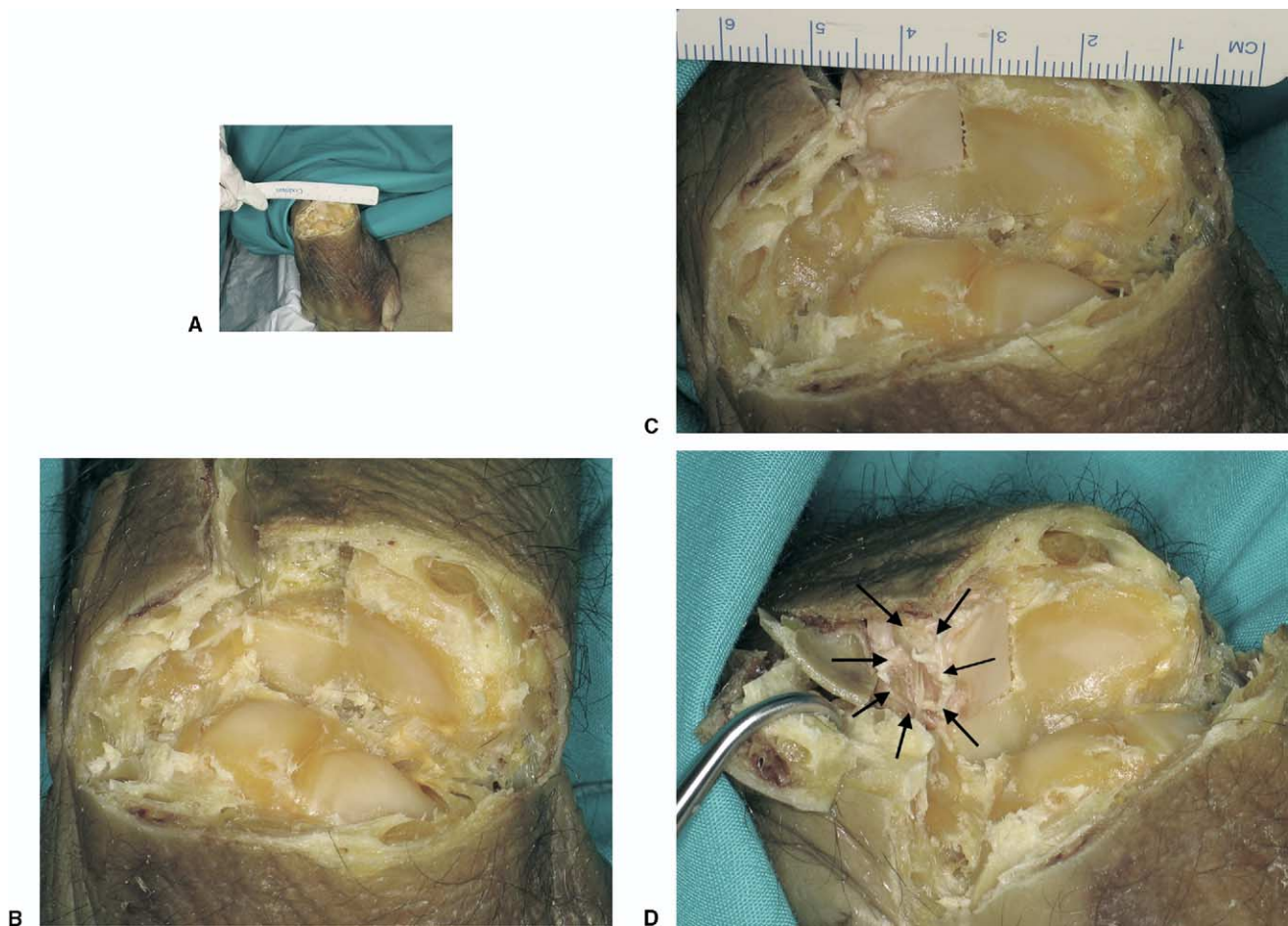


Figure 8. Simulation in a cadaver of the reconstruction of the malunited die-punch fragment. (A) All the dorsal structures have been divided sharply at the radiocarpal level and the wrist has been flexed to have an unimpeded view of the radius surface. (B) Close-up view in which the dorsal half of the right lunate facet of the distal radius has been resected in preparation for its reconstruction. (C, D) The dorsal half of the left third metatarsal is replacing the dorsal half of the lunate facet of the distal radius. It matches the radius slope in both views and the accessory facet (arrows) is located in a favorable position for reconstructing the sigmoid facet (when the contralateral metatarsal is selected).

early as 3 months after transplantation^{58,59} and the risk for viral transmission is higher. These techniques and others in which autologous osteochondral grafts are transplanted are indicated for central defects and are inappropriate when press-fit is not possible.^{12,60}

Autologous chondrocyte implantation has no risk for viral transmission as may occur with allografts nor are there donor-site complications as with osteochondral autografts, but it requires a uniform bone bed on which the chondrocytes can grow. Controversies exist as to the best way to deal with a cartilage surface defect, but this is beyond the scope of this article.^{20,21,61,62}

Perichondrium has been shown to generate hyaline cartilage.^{15,16} This technique has been used in the hand with variable success. It is applicable only to very limited problems in which damage is confined

to the cartilage and a healthy uniform bone surface is required.¹⁶⁻¹⁹ Conversely Thoma et al⁶³ failed to generate hyaline cartilage in a dog model with either a vascularized or nonvascularized perichondrial flap.

The type of articular defect presented in this article is not a single step-off in which an osteotomy plays a major role but a major irregularity after multifragmentation. Here only a piece of bone and cartilage could be used to restore the anatomy. Giachino et al² and Mehin et al³ presented a method to resurface the distal radius by means of an autologous osteochondral graft from the proximal tibiofibular joint with good results in 2 patients. Merrell et al⁴ found an indication for transferring a nonvascularized osteochondral graft that included all the scaphoid facet of the radius to reconstruct the sigmoid fossa.

Autogenous osteochondral grafts have been used profusely in the hand and the wrist particularly for

small bone defects.⁵⁻¹¹ Resorption has been noticed,⁵⁻⁷ and Ishida et al⁹ recommended the technique at the proximal interphalangeal joint for defects smaller than 50% of the head of the proximal phalanx to avoid massive resorption. Nevertheless larger defects including all the distal radius epiphysis have been replaced with a nonvascularized proximal head of the fibula with good results reported.^{64,65} Other investigators have found that the durability of the reconstruction was much better when the proximal fibula was transplanted, preserving its blood supply, and preferably if its epiphyseal nutrient vessels were included.^{36,37,66-68} The anatomic dissimilarities between the fibula and radius are marked.^{69,70} Consequently degeneration caused by incongruity is unavoidable in adults,^{67,68} rendering the transfer of living cartilage in that scenario worthless.

After consideration of feasible donor sites with minimal donor site morbidity we focused our anatomic studies on the base of the second and third metatarsals. The size of the base of the second metatarsal is quite similar to the third metatarsal; however, its surface is more irregular. This lack of evenness together with the fact that in 3 specimens the base of the second metatarsal was degenerated markedly with total wearing out of the cartilage made us disregard the base of the second metatarsal as a donor at present, focusing our attention on the third metatarsal (Appendices A and B can be viewed at the *Journal's* Web site, www.jhandsurg.org). The proximal facet of the third metatarsal has a fairly constant anatomy: a pear shape (wider dorsally than plantarly) with a flat surface slightly sloped plantarly and medially in the coronal plane. Conversely the blood supply is variable. The classic anatomic description of the dorsalis pedis artery with 3 lateral branches (proximal lateral tarsal artery, distal lateral tarsal artery, arcuate artery) is rare: it may represent less than 30%.⁷¹⁻⁷⁴ We found that the vision of Cormack and Lamberty⁷¹ of the anatomy of the dorsum of the foot closely matches our findings. They described a plexus where all the arteries are interrelated in a competitive fashion from where the dorsal intermetatarsal arteries originate (Fig. 2). In all specimens in our anatomic study we were able to track a periosteal artery to the dorsalis pedis and in all dried specimens the nutrient foramina could be found in the dorsum of the proximal aspect of the third metatarsal.

The distal radius articular facets have been studied in depth by Mekhail et al.⁷⁵ They found the scaphoid facet to be a triangle measuring 18 mm dorsal \times 16 mm palmar \times 13 mm ulnar, and the lunate facet to be

a polygon measuring 10 mm dorsal \times 13 mm lateral \times 14 mm palmar \times 15 mm ulnar. This anatomy matches quite well the proximal facet of the third metatarsal (12 mm dorsal \times 8 mm plantar \times 19 mm dorsoplantar) because it also is tilted slightly plantarward and tibialward. Additionally the third metatarsal has an accessory facet on its dorsofibular aspect: it has an average size of 8 \times 8 mm and is inclined plantarward and tibialward. The accessory facet can be used as the dorsal aspect of the sigmoid fossa (Tolat et al⁷⁶ types I and II) when reconstructing die-punch malunion (Fig. 8).

Graft harvesting is not easy for 2 reasons: the anatomic variability of the arterial network mentioned earlier and the fragility of the tiny periosteal vessels that may tear during dissection. It is important to preserve a cuff of periosteum to avoid a tear of these vessels. Exsanguination by elevation helps to define the arterial anatomy because it is mandatory to have a clear picture and to identify the vessels directed to the base of third metatarsal before ligation. Training on a cadaver is recommended strongly. Furthermore the procedure requires the sacrifice of the last portion of the dorsalis pedis artery. The presence of the posterior tibial artery should be ascertained with a Doppler probe before surgery. Microsurgical skills are required; however, the vessels are large.

The procedure presented is indicated for massive irreparable chondral defects of the radius. Although the result we have obtained is encouraging, at present this surgery should be considered preliminary.

The authors would like to acknowledge Professor F. Oñate, Chairman, Anatomy Department, University del Pais Vasco, Bilbao, Spain, and Robert Jenkins, PhD, for correcting the English version of this article.

References

1. Brittberg M, Peterson L, Sjogren-Jansson E, Tallheden T, Lindahl A. Articular cartilage engineering with autologous chondrocyte transplantation. A review of recent developments. *J Bone Joint Surg* 2003;85A(Suppl 3):109-115.
2. Giachino A, Mehin R, Backman D, Grabowski J. Autologous osteoarticular transfer from the proximal tibio-fibular joint to the distal radial facets in the treatment of severe distal radial fractures. *J Hand Surg* 2000;25B(Suppl 1):36.
3. Mehin R, Giachino AA, Backman D, Grabowski J, Fazekas A. Autologous osteoarticular transfer from the proximal tibiofibular joint to the scaphoid and lunate facets in the treatment of severe distal radial fractures: a report of two cases. *J Hand Surg* 2003;28A:332-341.
4. Merrell GA, Barrie KA, Wolfe SW. Sigmoid notch reconstruction using osteoarticular graft in a severely comminuted distal radius fracture: a case report. *J Hand Surg* 2002;27A:729-734.
5. Boulas HJ, Herren A, Büchler U. Osteochondral metatarsophal-

- langeal autografts for traumatic articular metacarpophalangeal defects: a preliminary report. *J Hand Surg* 1993;18A:1086–1092.
6. Boulas HJ. Autograft replacement of small joint defects in the hand. *Clin Orthop* 1996;327:63–71.
 7. Gaul JS Jr. Articular fractures of the proximal interphalangeal joint with missing elements: repair with partial toe joint osteochondral autografts. *J Hand Surg* 1999;24A:78–85.
 8. Hasegawa T, Yamano Y. Arthroplasty of the proximal interphalangeal joint using costal cartilage grafts. *J Hand Surg* 1992;17:583–585.
 9. Ishida O, Ikuta Y, Kuroki H. Ipsilateral osteochondral grafting for finger joint repair. *J Hand Surg* 1994;19A:372–377.
 10. Sandow MJ. Costo-osteochondral grafts in the wrist. *Tech Hand Upper Extrem Surg* 2001;5:165–172.
 11. Williams RMM, Kiefhaber TR, Sommerkamp TG, Stern PJ. Treatment of unstable dorsal proximal interphalangeal fracture/dislocations using a hemi-hamate autograft. *J Hand Surg* 2003;28A:856–865.
 12. Hangody L, Füles P. Autologous osteochondral mosaicplasty for the treatment of full-thickness defects of weight-bearing joints. Ten years of experimental and clinical experience. *J Bone Joint Surg* 2003;85A(Suppl 2):25–32.
 13. Shasha N, Krywulak S, Backstein D, Pressman A, Gross AE. Long-term follow-up of fresh tibial osteochondral allografts for failed tibial plateau fractures. *J Bone Joint Surg* 2003;85A(Suppl 2):33–39.
 14. Campbell CJ. Homotransplantation of half or whole joint. *Clin Orthop* 1972;87:146–155.
 15. Engkvist O, Johansson SH, Ohlén L, Skoog T. Reconstruction of articular cartilage using autologous perichondrial grafts. A preliminary report. *Scand J Plast Reconstr Surg* 1975;9:203–206.
 16. Johansson SH, Engkvist O. Small joint reconstruction by perichondrial arthroplasty. *Clin Plast Surg* 1981;8:107–114.
 17. Foucher G, Hoang P, Citron N, Merle M, Dury M. Joint reconstruction following trauma: comparison of microsurgical transfer and conventional methods: a report of 61 cases. *J Hand Surg* 1986;11B:388–393.
 18. Seradge H, Kutz JA, Kleinert HE, Lister GD, Wolff TW, Atasoy E. Perichondrial resurfacing arthroplasty in the hand. *J Hand Surg* 1984;9A:880–886.
 19. Takayama S, Nakao Y, Horiuchi Y, Itoh Y. Arthroplasty of MP and PIP joints using a chondroperichondrial graft. *Tech Hand Upper Extrem Surg* 1998;2:115–118.
 20. Knutsen G, Engebretsen L, Ludvigsen TC, Drogset JO, Grøntvedt T, Solheim E, et al. Autologous chondrocyte implantation compared with microfracture in the knee. A randomized trial. *J Bone Joint Surg* 2004;86A:455–464.
 21. Bentley G, Biant LC, Carrington RWJ, Akmal M, Goldberg A, Williams AM, et al. A prospective, randomised comparison of autologous chondrocyte implantation *versus* mosaicplasty for osteochondral defects in the knee. *J Bone Joint Surg* 2003;85B:223–230.
 22. Poole AR. What type of cartilage repair are we attempting to attain? *J Bone Joint Surg* 2003;85A(Suppl 2):40–44.
 23. Sledge C, Reddi AH, Walsh DA, Blake DR. Biology of the normal joint. In: Ruddy S, Harris ED Jr, Sledge CB, eds. *Kelley's textbook of rheumatology*. 6th ed. Philadelphia: Saunders, 2001:1–21.
 24. Simkin PA. The musculoskeletal system. In: Klippel JH, Dieppe PA, eds. *Rheumatology*. St. Louis: Mosby, 1994:1.2.1–1.2.10.
 25. Ulrich-Vinther M, Maloney MD, Schwarz EM, Rosier R, O'Keefe RJ. Articular cartilage biology. *J Am Acad Orthop Surg* 2003;11:421–430.
 26. Tsubokawa N, Yoshizu T, Maki Y. Long-term results of free vascularized second toe joint transfers to finger proximal interphalangeal joints. *J Hand Surg* 2003;28A:443–447.
 27. Dautel G, Gouzou S, Vialaneix J, Faivre S. PIP reconstruction with vascularized PIP joint from the second toe: minimizing the morbidity with the “dorsal approach and short-pedicle technique.” *Tech Hand Upper Extrem Surg* 2004;8:173–180.
 28. Entin MA, Alger JR, Baird RM. Experimental and clinical transplantation of autogenous whole joints. *J Bone Joint Surg* 1962;44A:1518–1536.
 29. Kettelkamp DB. Experimental autologous joint transplantation. *Clin Orthop* 1972;87:138–145.
 30. Planas J. Trasplante libre de articulaciones de los dedos. *Revista Española de Cirugía Plástica* 1968;1:21–30.
 31. Yoshizu T, Watanabe M, Tajima T. Étude expérimentale et applications cliniques des transferts libres d'articulation d'orteil avec anastomoses vasculaires. In: Tubiana R, ed. *Traité de chirurgie de la main*. Vol 2. Paris: Masson, 1984: 539–551.
 32. Imhof H, Sulzbacher I, Grampp S, Czerny C, Youssefzadeh S, Kainberger F. Subchondral bone and cartilage disease: a rediscovered functional unit. *Invest Radiol* 2000;35:581–588.
 33. Taylor GI, Miller GDH, Ham FJ. The free vascularized bone graft. A clinical extension of microvascular techniques. *Plast Reconstr Surg* 1975;55:533–544.
 34. Taylor GI, Townsend P, Corlett R. Superiority of the deep circumflex iliac vessels as the supply for free groin flaps. Clinical work. *Plast Reconstr Surg* 1979;64:745–759.
 35. Tsai T-M, Ludwig L, Tonkin M. Vascularized fibular epiphyseal transfer. A clinical study. *Clin Orthop* 1986;210: 228–234.
 36. Taylor GI, Wilson KR, Rees MD, Corlett RJ, Cole WG. The anterior tibial vessels and their role in epiphyseal and diaphyseal transfer of the fibula: experimental study and clinical applications. *Br J Plast Surg* 1988;41:451–469.
 37. Innocenti M, Delcroix L, Manfrini M, Ceruso M, Capanna R. Vascularized proximal fibular epiphyseal transfer for distal radial reconstruction. *J Bone Joint Surg* 2004;86A:1504–1511.
 38. Zaidenberg C, Siebert JW, Angrigiani C. A new vascularized bone graft for scaphoid nonunion. *J Hand Surg* 1991; 16A:474–478.
 39. Moran SL, Cooney WP, Berger RA, Bishop AT, Shin AY. The use of the 4 + 5 extensor compartmental vascularized bone graft for the treatment of Kienböck's disease. *J Hand Surg* 2005;30A:50–58.
 40. Taylor GI, Palmer JH. The vascular territories (angiosomes) of the body: experimental study and clinical applications. *Br J Plast Surg* 1987;40:113–141.
 41. Taylor GI, Caddy CM, Watterson PA, Crock JG. The venous territories (venosomes) of the human body: experimental study and clinical implications. *Plast Reconstr Surg* 1990; 86:185–213.
 42. Failla JM. Hook of hamate vascularity: vulnerability to osteonecrosis and nonunion. *J Hand Surg* 1993;18A:1075–1079.
 43. Garcia-Elias M, Lluch A, Ferreres A, Papini-Zorli I, Rahimtoola ZO. Treatment of radiocarpal degenerative osteoarthritis

- by radioscapholunate arthrodesis and distal scaphoidectomy. *J Hand Surg* 2005;30A:8–15.
44. Rosales RS, Delgado EB, Diez de la Lastra-Bosch I. Evaluation of the Spanish version of the DASH and carpal tunnel syndrome health-related quality-of-life instruments: cross-cultural adaptation process and reliability. *J Hand Surg* 2002;27A:334–343.
 45. Maloney CT Jr, DeJesus R, Dellon AL. Painful foot neuromas after toe-to-thumb transfer. *J Hand Surg* 2005;30A:105–110.
 46. Espinar Salom E. Sistemas de valoración de los resultados clínicos en la cirugía del pie. In: Núñez-Samper Pizarroso M, Llanos-Alcázar LF, Viladot Pericé R, eds. *Técnicas quirúrgicas de cirugía del pie*. Barcelona: Masson, 2003:361–370.
 47. Knirk JL, Jupiter JB. Intra-articular fractures of the distal end of the radius in young adults. *J Bone Joint Surg* 1986;68A:647–659.
 48. Wagner WF Jr, Tencer AF, Kiser P, Trumble TE. Effects of intra-articular distal radius depression on wrist joint contact characteristics. *J Hand Surg* 1996;21A:554–560.
 49. Fernandez DL. Reconstructive procedures for malunion and traumatic arthritis. *Orthop Clin North Am* 1993;24:341–363.
 50. González del Pino J, Nagy L, González Hernandez E, Bartolome del Valle E. Osteotomías intraarticulares complejas del radio por fractura. Indicaciones y técnica quirúrgica. *Revista de Ortopedia y Traumatología* 2000;44:406–417.
 51. Marx RG, Axelrod TS. Intraarticular osteotomy of distal radius malunions. *Clin Orthop* 1996;327:152–157.
 52. Ring D, Prommersberger K-J, Gonzalez del Pino J, Capomassi M, Shullitel M, Jupiter JB. Corrective osteotomy for intra-articular malunion of the distal part of the radius. *J Bone Joint Surg Am* 2005;87A:1503–1509.
 53. Saffar P. Radio-lunate arthrodesis for distal radial intra-articular malunion. *J Hand Surg* 1996;21B:14–20.
 54. Nagy L, Büchler U. Long-term results of radioscapholunate fusion following fractures of the distal radius. *J Hand Surg* 1997;22B:705–710.
 55. Garcia-Elias M, Lluch A. Partial excision of scaphoid: is it ever indicated? *Hand Clin* 2001;17:687–695.
 56. McCombe D, Ireland DCR, McNab I. Distal scaphoid excision after radioscaphoid arthrodesis. *J Hand Surg* 2001;26A:877–882.
 57. Maruyama S, Hasegawa Y, Sakano S, Warashina H, Kitamura S, Yamauchi K, Iwata H. Experimental evaluation of the usefulness of osteochondral allograft for articular cartilage defect. *J Orthop Sci* 2003;8:560–566.
 58. Kandel RA, Pritzker KPH, Langer F, Gross AE. The pathologic features of massive osseous grafts. *Hum Pathol* 1984;15:141–146.
 59. Oakeshott RD, Farine I, Pritzker KPH, Langer F, Gross AE. A clinical and histologic analysis of failed fresh osteochondral allografts. *Clin Orthop* 1988;233:283–294.
 60. Palazzi Coll S, Palazzi Coll C, Palazzi Duarte A-S. Osteochondral autograft of the knee. *Int Orthop* 1977;1:48–52.
 61. Kish G, Hangody L. Comment on: A prospective, randomised comparison of autologous chondrocyte implantation *versus* mosaicplasty for osteochondral defects in the knee. *J Bone Joint Surg* 2004;86B:619.
 62. LaPrade RF. Comment on: Autologous chondrocyte implantation was superior to mosaicplasty for repair of articular cartilage defects in the knee at one year. *J Bone Joint Surg* 2003;85A:2259.
 63. Thoma A, Dunlop B, Orr FW, Payk I, Adachi JD. Perichondrial arthroplasty in a canine elbow model: comparison of vascularized and nonvascularized techniques. *Plast Reconstr Surg* 1991;91:307–315.
 64. Harness NG, Mankin HJ. Giant-cell tumor of the distal forearm. *J Hand Surg* 2004;29A:188–193.
 65. Mack GR, Lichtman DM, MacDonald RI. Fibular autografts for distal defects of the radius. *J Hand Surg* 1979;4:576–583.
 66. Ferracini R, Gino G, Battiston B, Linari A, Franz R, Bertolo S. Assessment of vascularized fibular graft one year after reconstruction of the wrist after excision of a giant-cell tumour. *J Hand Surg* 1999;24B:497–500.
 67. Minami A, Kato H, Iwasaki N. Vascularized fibular graft after excision of giant-cell tumor of the distal radius: wrist arthroplasty versus partial wrist arthrodesis. *Plast Reconstr Surg* 2002;110:112–117.
 68. Ono H, Yajima H, Mizumoto S, Miyauchi Y, Mii Y, Tamai S. Vascularized fibular graft for reconstruction of the wrist after excision of giant cell tumor. *Plast Reconstr Surg* 1997;99:1086–1093.
 69. Ogden JA. The anatomy and function of the proximal tibiofibular joint. *Clin Orthop* 1974;101:186–191.
 70. Ogden JA. Subluxation of the proximal tibiofibular joint. *Clin Orthop* 1974;101:192–197.
 71. Cormack GC, Lamberty BG. Lower leg. In: Cormack GC, Lamberty BGH, eds. *The arterial anatomy of skin flaps*. 2nd ed. Edinburgh: Churchill Livingstone, 1994:248–267.
 72. Gilbert BJ, Horst F, Nunley JA. Potential donor rotational bone grafts using vascular territories in the foot and ankle. *J Bone Joint Surg* 2004;86A:1857–1873.
 73. Huber JF. The arterial network supplying the dorsum of the foot. *Anat Rec* 1941;80:373–391.
 74. Yamada T, Gloviczki P, Bower TC, Naessens JM, Carmichael SW. Variations of the arterial anatomy of the foot. *Am J Surg* 1993;166:130–135.
 75. Mekhail AO, Ebraheim NA, McCreath WA, Jackson WT, Yeasting RA. Anatomic and X-ray film studies of the distal articular surface of the radius. *J Hand Surg* 1996;21A:567–573.
 76. Tolat AR, Stanley JK, Trail IA. A cadaveric study of the anatomy and stability of the distal radioulnar joint in the coronal and transverse planes. *J Hand Surg* 1996;21B:587–594.

Appendix A. Mean, Minimum, and Maximum Values of Parameters Measured at the Second Metatarsal Bases of 20 Specimens (Values in mm)

Parameters	Mean	Minimum	Maximum
Dorsoplantar length	19.1	16	22
Width of dorsal aspect	13.3	11	17
Width of plantar aspect	7.9	6	10
Inflexion point (from dorsal aspect)	8.8	6	11
Dorsofibular facet DP+	5.7	5	7
Dorsofibular facet PD++	9.6	6	12
Plantofibular facet DP+	7.1	4	11
Plantofibular facet PD++	5.8	3	10
Tibial facet DP+	4.0	3	6
Tibial facet PD++	4.2	3	6
Articular area (mm ²)	184.6	121	246

+ PD, Proximal-to-distal; ++ DP, Dorsal-to-plantar.

Appendix B. Detail of the Findings in Each Specimen Studied in This Work (Measures in mm)

	1	2	3	4	5	6	7	8
Age, y	60	60	24	24	30	30	86	86
Dorsalis pedis artery diameter	2.2	1.8	2.2	2.2	2	1.5	2.8	2
Arcuate artery diameter	0.7	0.8	0.5	0.4	0.2	—	0.5	—
Distal lateral tarsal artery diameter	0.5	0.5	0.7	0.5	0.5	0.5	0.6	1
Arcuate to third CMT*	6	15	12	9	4	—	15	—
DLTA to third CMT†	22	15	22	23	19	22	15	22
Third metatarsal parameters								
Dorsoplantar length	21	20	21	21	19	19	18	19.5
Width of dorsal aspect	14	14	15	14	11	11	11	12
Width of plantar aspect	8	9	9	8	8	8	7	7
Inflexion point (from dorsal aspect)	9	9	10	9	9	7	8	9
Articular area (mm ²)	205	189	212	206	152	153	138	145
Dorsotibial facet DP+	6	5	5	7	4	6	6	6
Dorsotibial facet PD++	6	5	5	7	6	6	6	5
Plantotibial facet DP+	—	—	4	6	7	7	7	7
Plantotibial facet PD++	—	—	4	6	2	4	5	5
Fibular facet DP+	7	7	8	7	7	8	10	8
Fibular facet PD++	8	9	10	11	7	8	7	9
Tolat type	II	II	II	II	II	II	II	II
Shape of the proximal facet	Concave	Concave	Flat	Flat	Flat	Concave	Flat	Flat
Tibial tilt	10°	6°	10°	6°	3°	5°	3°	10°
Plantar tilt	3°	5°	3°	3°	4°	5°	3°	7°
Degenerative findings	—	—	—	—	—	—	—	—
Second metatarsal parameters								
Dorsoplantar length	18	18	20	20	20	20	17	16
Width of dorsal aspect	16	15	13	13	12	12	12	12
Width of plantar aspect	8	8	7	8	10	8	7	8
Inflexion point (from dorsal aspect)	8	8	9	10	10	9	8	9
Articular area (mm ²)	211	216	192	208	163	170	171	140
Dorsofibular facet DP+	5	7	5	7	6	5	6	6
Dorsofibular facet PD++	11	11	10	11	9	12	7	8
Plantofibular facet DP+	6	7	6	6	7	6	8	5
Plantofibular facet PD++	5	5	6	5	5	5	3	4
Tibial facet DP+	—	3	—	—	—	3	—	3
Tibial facet PD++	—	3	—	—	—	3	—	3
Shape of the proximal facet	Concave	Concave	Concave	Concave	Concave	Concave	Concave	Concave
Tibial tilt	3°	4°	3°	6°	15°	2°	1°	2°
Plantar tilt	4°	5°	4°	3°	3°	7°	5°	6°
Degenerative findings	—	—	—	—	—	—	—	—

DLTA, distal lateral tarsal artery; +PD, proximal-to-distal; ++DP, dorsal-to-plantar.

*Distance from the arcuate artery to the third cuneometatarsal joint.

†Same from the distal lateral tarsal artery. Note that the take-off of the distal lateral tarsal artery always is proximal.

